Rock-Support Interaction analysis for tunnels in weak rock masses

Introduction

Tunnelling in weak rock presents some special challenges to the geotechnical engineer since misjudgements in the design of support systems can lead to very costly failures. In order to understand the issues involved in the process of designing support for this type of tunnel it is necessary to examine some simple basic concepts of how a rock mass surrounding a tunnel deforms and how the support systems acts to control this deformation. This Rock-Support Interaction or Convergence-Confinement analysis is limited to circular tunnels in an in-situ stress field in which all three principal stresses are equal and where the rock mass exhibits elastic-perfectly plastic shear failure. It should not be used for the detailed design of tunnels in more complex rock masses and in-situ stress fields. More comprehensive analyses are available for these situations (Hoek et al, 2008).

Deformation around an advancing tunnel

Figure 1 shows the results of a three-dimensional finite element analysis of the deformation and failure of the rock mass surrounding a circular tunnel advancing through a weak rock mass subjected to equal stresses in all directions. The plot shows displacement vectors in the rock mass, the shape of the deformed tunnel profile and the shape of the plastic zone surrounding the tunnel. Figure 2 gives a graphical summary or the most important features of this analysis.

Elastic deformation of the rock mass starts about two diameters ahead of the advancing face and reaches its maximum value at about two diameters behind the face. At the face position about one third of the total radial closure of the tunnel has already occurred and the tunnel face deforms inwards as illustrated in Figures 1 and 2. Whether or not these deformations induce stability problems in the tunnel depends upon the ratio of rock mass strength to the in situ stress level, as will be demonstrated in the following pages.

Note that it is assumed that deformation process described occurs immediately upon excavation of the face. This is a reasonable approximation for most tunnels in rock. The effects of time dependent deformations upon the performance of the tunnel and the design of the support system will be not be discussed in this chapter.

Tunnel deformation analysis

In order to explore the concepts of rock support interaction in a form which can readily be understood, a very simple analytical model based on the Mohr-Coulomb failure criterion will be utilised. This model involves a circular tunnel subjected to a hydrostatic stress field in which the horizontal and vertical stresses are equal.

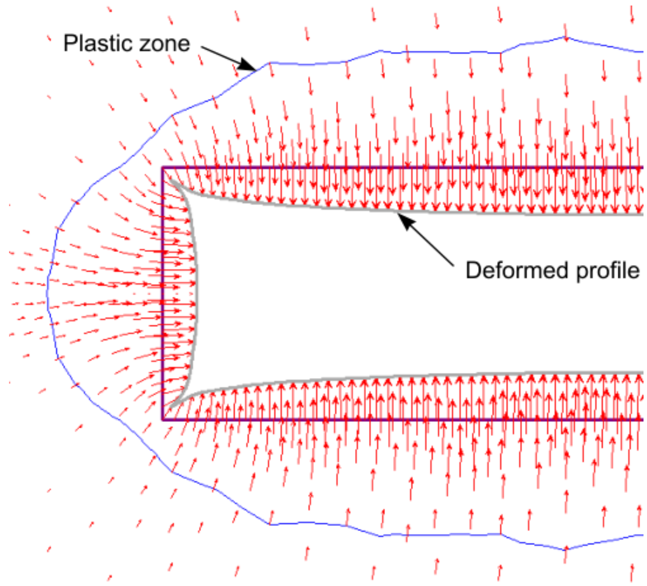

Figure 1: Vertical section through an axi-symmetric three-dimensional finite element model of the failure and deformation of the rock mass surrounding the face of an advancing circular tunnel. The plot shows displacement vectors as well as the shape of the deformed tunnel profile.

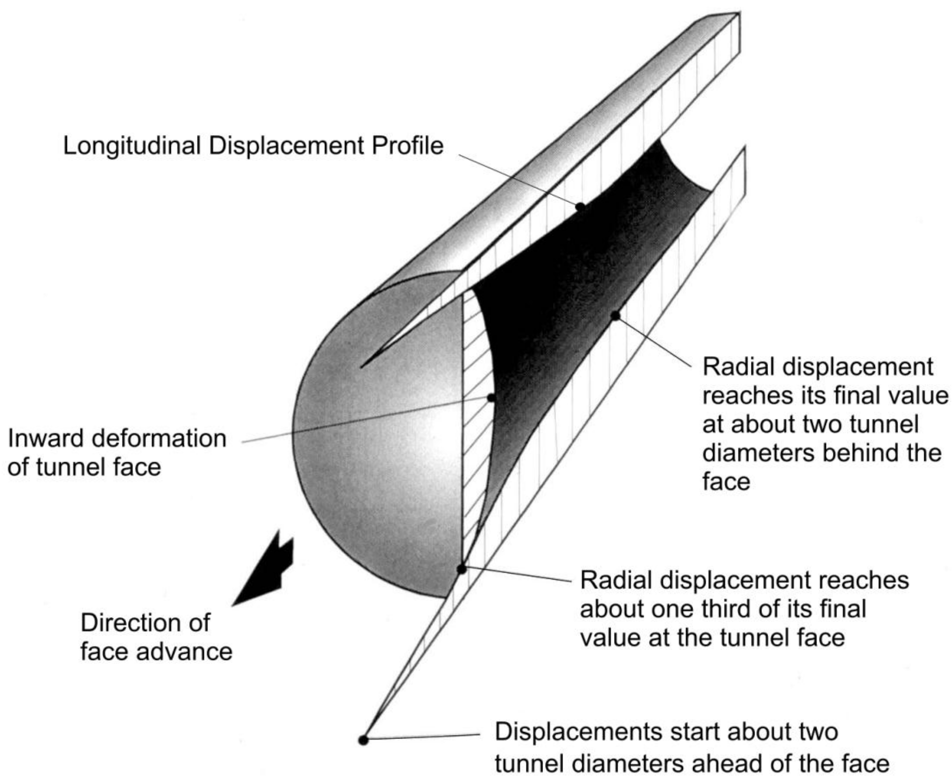

Figure 2: Pattern of elastic deformation in the rock mass surrounding an advancing tunnel.

Rock-support interaction analysis for tunnels

In this analysis it is assumed that the surrounding homogeneous weak rock mass behaves as an elastic-perfectly plastic material in which failure involving slip along closely spaced intersecting discontinuities is assumed to occur with zero plastic volume change (Duncan Fama, 1993).

Definition of failure criterion

It is assumed that the onset of plastic failure, for different values of the effective confining stress $\sigma_3^{'}$, is defined by the Mohr-Coulomb criterion and expressed as:

$$\sigma_1^{'} = \sigma_{cm} + k\sigma_3^{'} \tag{1}$$

The uniaxial compressive strength of the rock mass σ_{cm} is defined by:

$$\sigma_{cm} = \frac{2c^{'}\cos\phi^{'}}{(1-\sin\phi^{'})} \tag{2}$$

and the slope k of the $\sigma_1^{'}$ versus $\sigma_3^{'}$ plot as:

$$k = \frac{(1+\sin\phi^{'})}{(1-\sin\phi^{'})} \tag{3}$$

where $\sigma_1^{'}$ is the axial stress at which failure occurs
$\sigma_3^{'}$ is the confining stress
$c^{'}$ is the cohesive strength and
$\phi^{'}$ is the angle of friction of the rock mass

Analysis of tunnel behaviour

Assume that a circular tunnel of radius r_o is subjected to hydrostatic stresses p_o and a uniform internal support pressure p_i as illustrated in Figure 3. Failure of the rock mass surrounding the tunnel occurs when the internal pressure p_i is less than a critical support pressure p_{cr}, which is defined by:

$$p_{cr} = \frac{2p_o - \sigma_{cm}}{1+k} \tag{4}$$

If the internal support pressure p_i is greater than the critical support pressure p_{cr}, no failure occurs, the behaviour of the rock mass surrounding the tunnel is elastic and the inward radial elastic displacement u_{ie} of the tunnel wall is given by:

$$u_{ie} = \frac{r_o(1+\nu)}{E_m}(p_o - p_i) \quad (5)$$

where E_m is the Young's modulus or deformation modulus and
ν is the Poisson's ratio of the rock.

When the internal support pressure p_i is less than the critical support pressure p_{cr}, failure occurs and the radius r_p of the plastic zone around the tunnel is given by:

$$r_p = r_o\left[\frac{2(p_o(k-1)+\sigma_{cm})}{(1+k)((k-1)p_i+\sigma_{cm})}\right]^{\frac{1}{(k-1)}} \quad (6)$$

For plastic failure, the inward radial displacement u_{ip} of the walls of the tunnel is:

$$u_{ip} = \frac{r_o(1+\nu)}{E}\left[2(1-\nu)(p_o - p_{cr})\left(\frac{r_p}{r_o}\right)^2 - (1-2\nu)(p_o - p_i)\right] \quad (7)$$

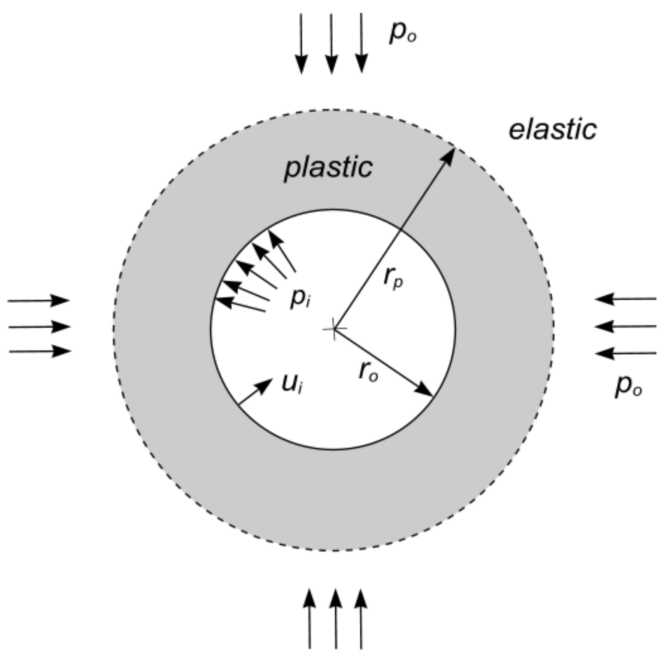

Figure 3: Plastic zone surrounding a circular tunnel.

Characteristic curve for a tunnel

Equations 4 to 7, presented above, define the relationship between internal support pressure p_i and the tunnel deformation u_i for an advancing circular tunnel in a hydrostatic stress field. A plot of u_i versus p_i is generally known as the *Characteristic Curve* for the tunnel and an example is given in Figure 4. This curve is based on the assumption that the rock at the tunnel face provides an initial support pressure equal to the in situ stress p_o. As the tunnel face advances and the face moves away from the section under consideration, the support pressure gradually decreases until it reaches zero at some distance behind the face. Also included in Figure 4 is the radius of the plastic zone r_p, calculated from equation 6.

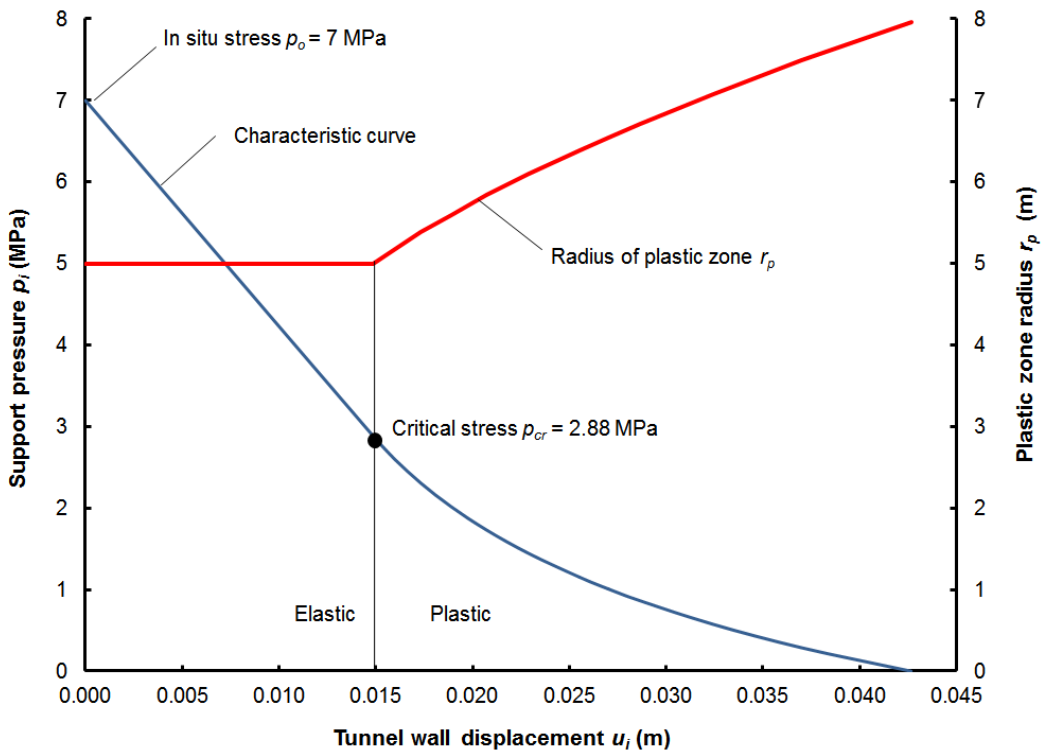

Input:	Output:
Tunnel radius r_o = 5 m	Rock mass UCS σ_{cm} = 4.53 MPa
Friction angle ø = 23°	Rock mass constant k = 2.28
Cohesion c = 1.5 MPa	Critical pressure p_{cr} = 2.88 MPa
Modulus E = 1800 MPa	Max tunnel displacement = 0.0427 m
Poisson's ratio ν = 0.3	Max plastic zone radius = 7.96 m
In situ stress p_o = 7 MPa	Plastic zone/tunnel radius = 1.592

Figure 4: Characteristic curve for a tunnel excavated in weak rock.

Longitudinal Displacement Profile

The calculation of the characteristic curve and the extent of the plastic zone are based on a two-dimensional analysis as shown in Figure 3. The Longitudinal Displacement Profile, shown in Figure 2, is required in order to establish the relative position of the tunnel face and the sections under consideration. It is necessary to carry out a three-dimensional analysis to determine this profile. The results of such a study have been published by Vlachopoulos and Diederichs (2009) and are summarized in Figure 5.

The Longitudinal Displacement Profile for a specific tunnel is calculated as follows:

The ratio of maximum plastic zone radius r_{pm} to the tunnel radius $r_{o,}$ is calculated from equation 6 by setting pi = 0:

$$\frac{r_{pm}}{r_o} = \left[\frac{2(p_o(k-1)+\sigma_{cm})}{(1+k)\sigma_{cm}} \right]^{\frac{1}{(k-1)}} \quad (8)$$

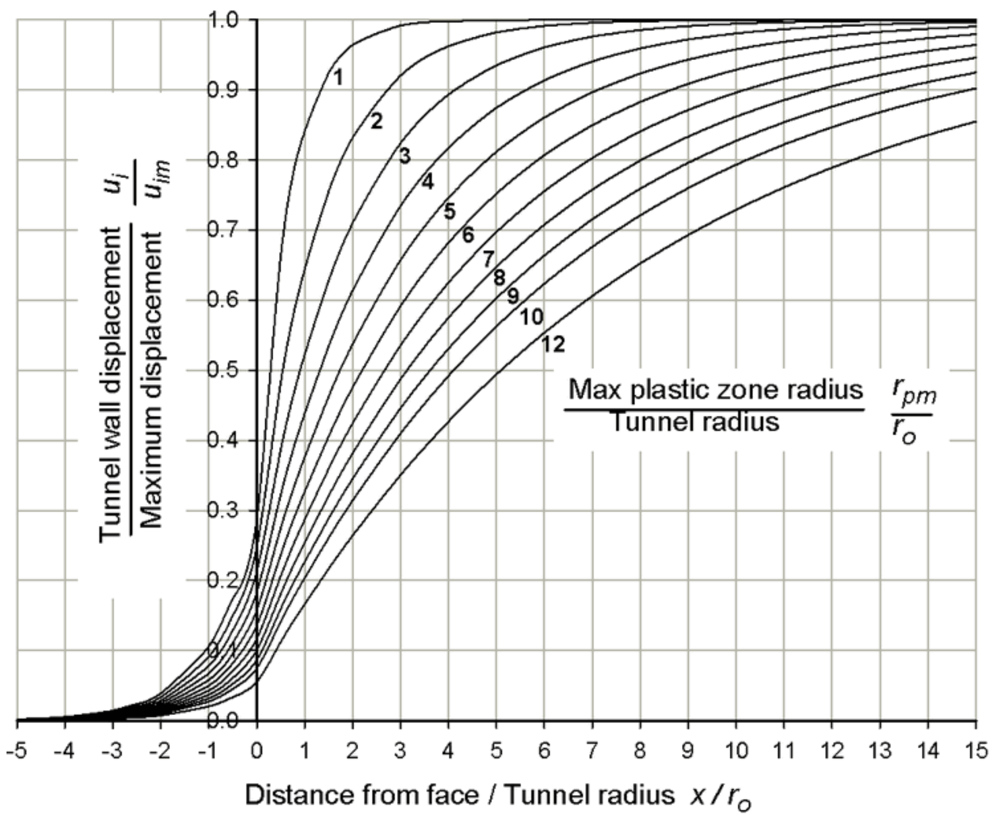

Figure 5: Longitudinal Displacement Profile (After Vlachopoulos and Diederichs, 2009).

The displacement at the tunnel face u_{if} is calculated from the following equation derived by Vlachopoulos and Diederichs:

$$u_{if} = \left(\frac{u_{im}}{3}\right) e^{-0.15(r_{pm}/r_o)} \tag{9}$$

where u_{im} is the maximum displacement which occurs at r_{pm}.

The tunnel wall displacement ahead of the face ($x < 0$) is:

$$u_i = \frac{u_{if}}{u_{im}} . e^{x/r_o} \tag{10}$$

The tunnel wall displacement behind the face ($x > 0$) is:

$$u_i = 1 - \left(1 - \frac{u_{if}}{u_{im}}\right) . e^{\left(-3x/r_o\right)/\left(2r_{pm}/r_o\right)} \tag{11}$$

A Longitudinal Displacement Profile for a typical tunnel is plotted in Figure 6.

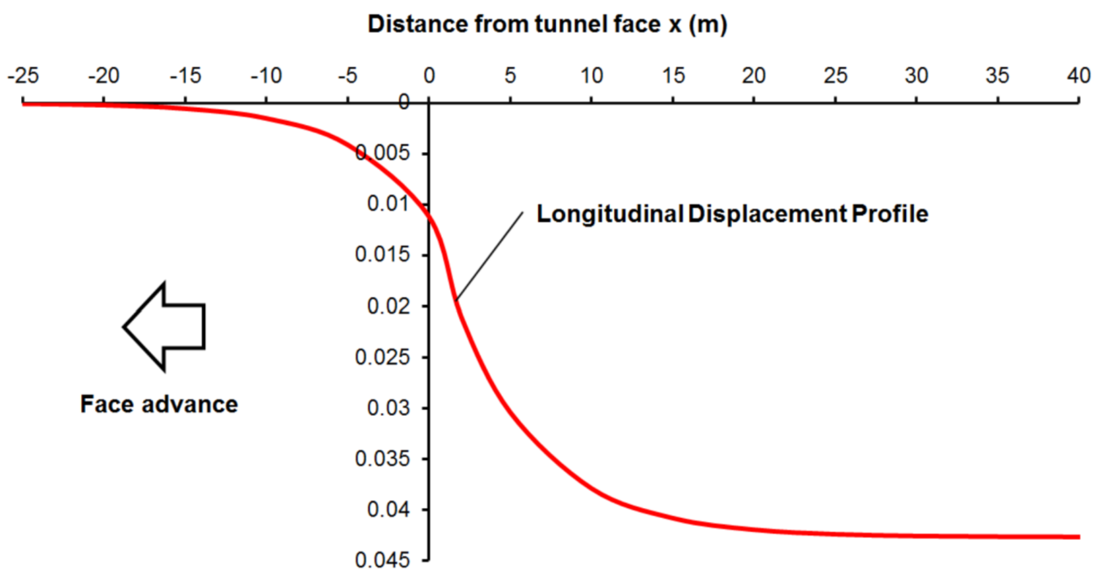

Input:	Output:
Tunnel radius r_o = 5 m	Max plastic zone/tunnel radius r_{pm}/r_o = 1.592
In situ stress p_o = 7 MPa	Tunnel face displacement u_{if} = 0.011197 m
Rock mass UCS σ_{cm} = 4.53 MPa	Maximum tunnel displacement u_{im} = 0.0427 m
Rock mass constant k = 2.28	Face displacement/Max displacement u_{if}/u_{im} = 0.2622

Figure 6: Longitudinal Displacement Profile for tunnel considered in Figure 4.

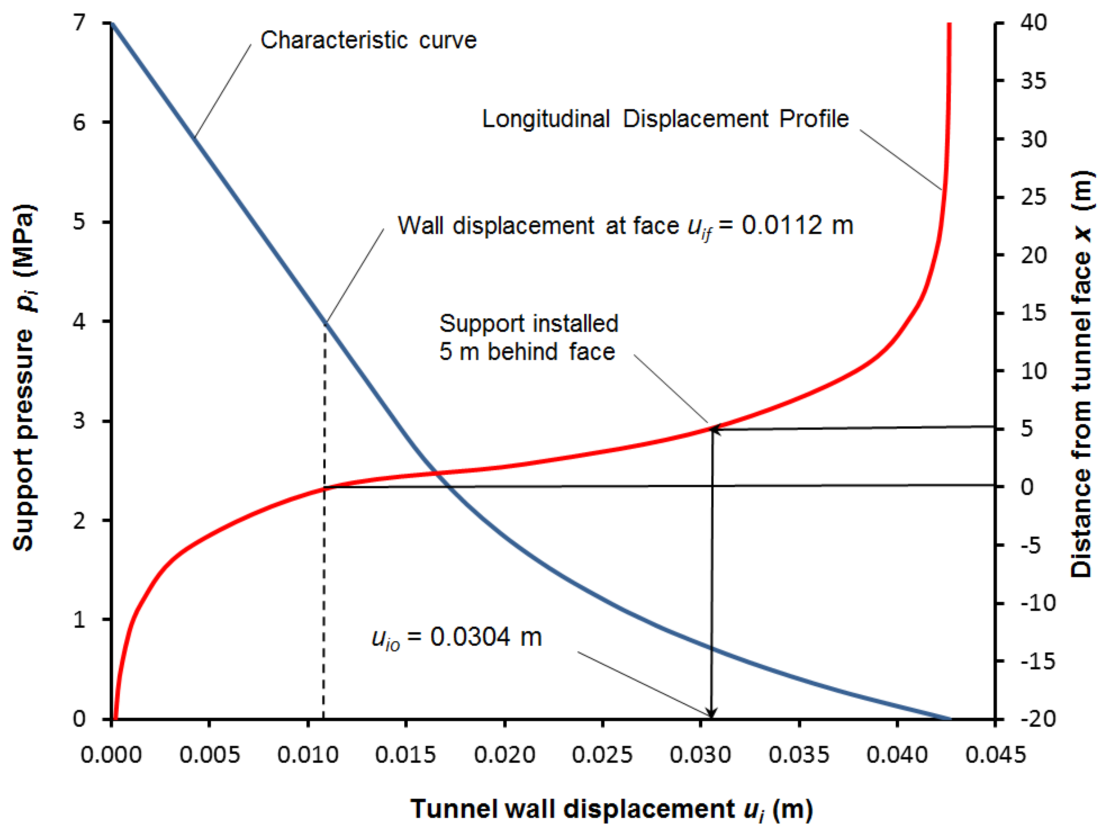

Figure 7: Combined Characteristic Curve and Longitudinal Displacement Profile plot.

Combining the Characteristic Curve from Figure 4 and the Longitudinal Displacement Profile from Figure 6, as was done by Carranza-Torres and Fairhurst (2000), gives the plot presented in Figure 7. This plot allows the tunnel wall displacement at a given distance behind the face to be determined. Hence, as shown in Figure 7, support installed 5 m behind the face will correspond to a tunnel wall displacement u_i = 0.0304 m and the support required to stabilize the tunnel is of the order of 0.6 MPa.

Rock-Support interaction

As shown by equations 6 and 7 above, the extent of the plastic or failure zone and the amount of deformation in the rock mass surrounding the tunnel can be controlled by the application of an internal support pressure p_i. This support can be provided by combinations of rockbolts, steel sets and shotcrete or concrete linings. The interaction of the deforming rock mass and the resisting support can be illustrated in the plot given in Figure 8.

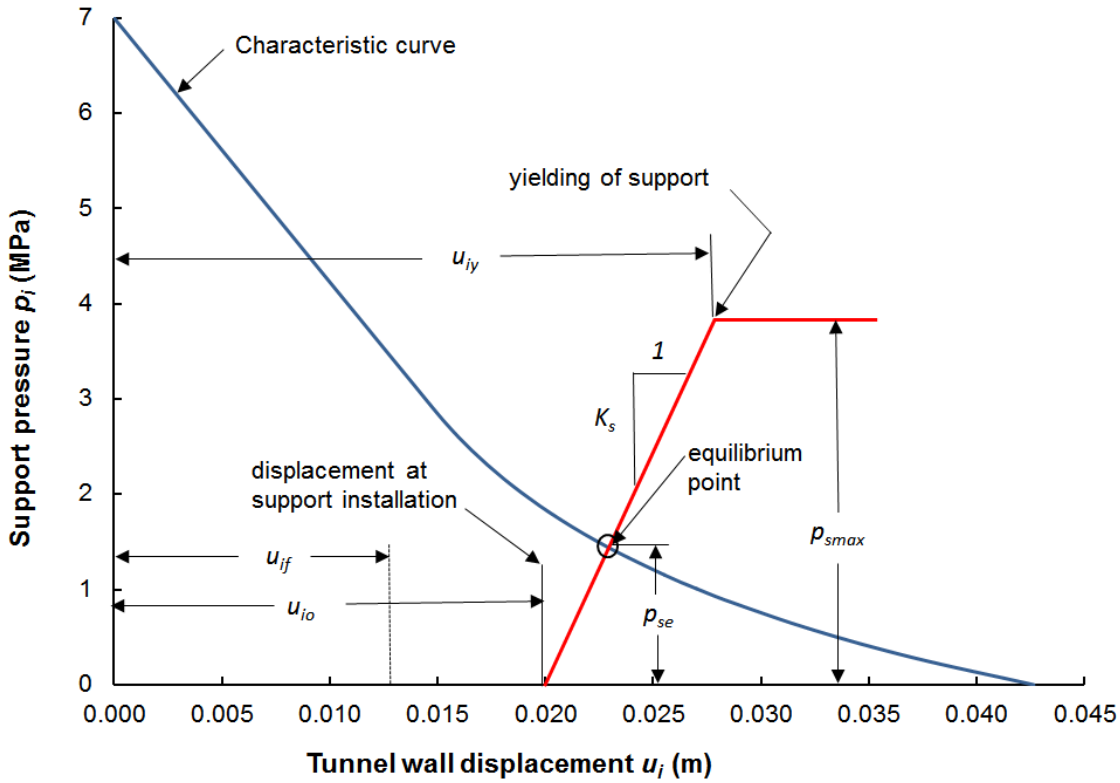

Figure 8: Rock-Support interaction plot.

Assuming that the support is installed at some distance behind the tunnel face, the displacement at this distance u_{io} is determined from Figure 7. The reaction of the installed support to on-going deformation depends upon the stiffness K_s of the support system and, as shown in Figure 8, the displacement u_{iy} of the support at yield is given by

$$u_{iy} = u_{io} + \frac{p_{smax}}{K_s} \tag{12}$$

where p_{smax} is the capacity of the support and r_o is the radium of the tunnel.
If the support has sufficient capacity the rock-support intersection curve will intersect the characteristic curve of the tunnel at an equilibrium point where the deformation of the tunnel equals that of the support. The factor of safety (FS) of the support is then defined as the ratio of capacity to demand or

$$FS = \frac{p_{smax}}{p_{se}} \tag{13}$$

Estimation of support capacity

Hoek and Brown (1980a) and Brady and Brown (1985) published equations calculating the capacity of steel sets, shotcrete or concrete linings and rockbolts for a circular tunnel in a hydrostatic stress field.

An error in the equation for the support capacity of blocked steel sets[1] resulted in an overestimate of the support capacity of sets with very small block spacings, used to estimate the capacity of steel sets backing onto shotcrete or embedded in shotcrete. In many current tunnelling operations, particularly in TBM bored tunnels, the steel sets are placed in direct contact with the rock or with shotcrete used to backfill overbreak. Consequently, the equation for estimating the support capacity of steel sets has been simplified to that for sets in direct contact with the rock as illustrated in Figure 9

Steel set support

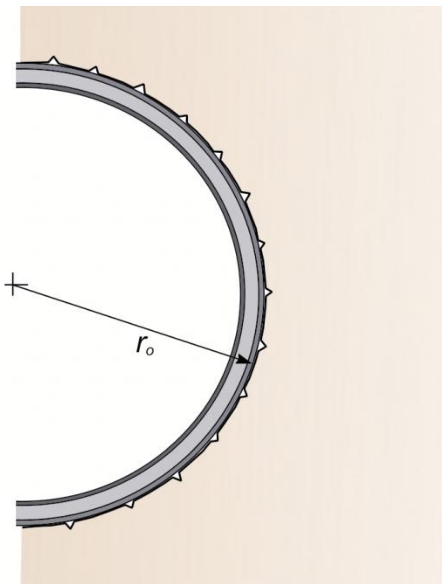

σ_{ys} is the yield strength of the steel (MPa)
E_s is the Young's modulus of the steel (MPa)
A_s is the cross-sectional area of the section (m^2)
s_l is the set spacing along the tunnel axis (m)
r_o is the radius of the tunnel (m)

Figure 9 : Steel set support

The maximum support pressure p_{ssmax} of the sets is

$$p_{ssmax} = \frac{A_s \sigma_{ys}}{s_l r_o} \tag{14}$$

The stiffness K_{ss} of the sets is

$$K_{ss} = \frac{E_s A_s}{s_l r_o^2} \tag{15}$$

[1] This error was pointed out by Mr Alex Lowson of Mott MacDonald who provided a corrected version of the equation. He also suggested that, in the context of this discussion, it was probably more appropriate to assume that the steel set is directly in contact with the rock surface or with a shotcrete layer used to fill overbreaks as shown in Figure 9.

Concrete or shotcrete linings

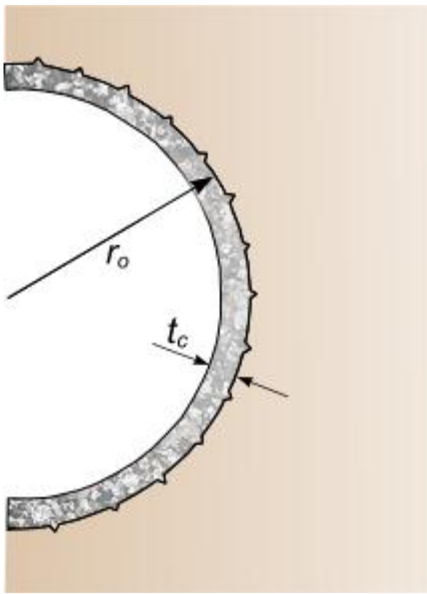

σ_{cc} is the uniaxial compressive strength of the concrete of shotcrete (MPa)
E_c is the Young's modulus of the concrete or shotcrete (MPa)
ν_c is the Poisson's ratio of the concrete of shotcrete
t_c is the thickness of the lining (m)
r_o is the radius of the tunnel (m)

Figure 10: Shotcrete support

The maximum support pressure p_{scmax} is

$$p_{scmax} = \frac{\sigma_{cc}}{2}\left[1 - \frac{(r_o - t_c)^2}{r_o^2}\right] \tag{16}$$

The stiffness K_{sc} is

$$K_{sc} = \frac{E_c(r_o^2 - (r_o - t_c)^2)}{2(1 - \nu^2)(r_o - t_c)r_o^2} \tag{17}$$

Rockbolts

The action of rockbolts and cables installed in the rock mass surrounding a tunnel can be complex. For example, fully grouted rockbolts act as reinforcement of the rock in much the same way as reinforcing steel acts in concrete. As a result they change the shape of the characteristic curve rather than provide internal support equivalent to that given by steel sets or shotcrete linings. On the other hand, ungrouted anchored rockbolts can be considered to resist the inward displacement of the rock mass and this is equivalent to the application of an internal support pressure in the tunnel.

For the sake of simplicity the following analysis is limited to the support provided by ungrouted mechanically or chemically anchored rockbolts or cables. More detailed numerical analyses of the interaction of rockbolts and failing rock masses are provided in other chapters in these notes.

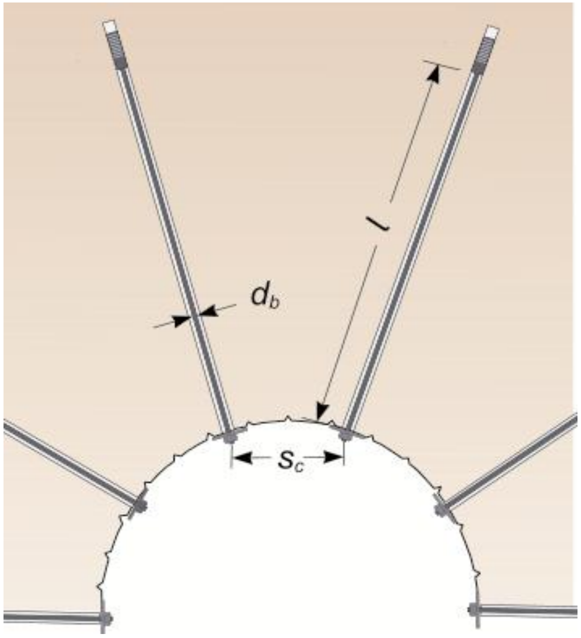

d_b is the rockbolt or cable diameter (m)
l is the free length of the bolt or cable (m)
E_s is the Young's modulus of the bolt or cable (MPa)
s_c is the circumferential bolt spacing (m)
s_l is the longitudinal bolt spacing (m)
T_{bf} is the ultimate bolt or cable load obtained from a pull-out test (MN)

Figure 11: Ungrouted rockbolt support

The maximum support pressure provided by a rockbolt pattern is

$$p_{sbmax} = \frac{T_{bf}}{s_l s_c} \tag{18}$$

The elastic stiffness is

$$K_{sb} = \frac{E_s \pi d_b^2}{4l\ s_l s_c} \tag{19}$$

In applying equations 18 and 19 in a convergence-confinement analysis it is assumed that the rockbolts or cables are installed in a uniform pattern in the rock mass surrounding the tunnel. The length l of the bolts or cables should exceed the thickness of the plastic zone around the tunnel and the spacing s_c and s_l of the bolts should generally be less than half the bolt length.

Plot of maximum support pressures versus tunnel diameter

Figure 12a gives a range of typical support types used in tunnelling and the maximum support pressures for these support types are plotted in Figure 12b, for a range of tunnel radii.

Support type	Section depth - m	Flange width m	Sectional area m^2	Weight – kg/m	Curve number	Designation Metric/Imperial
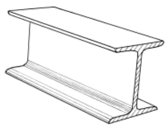 Wide flange rib	0.307 0.216 0.162	0.305 0.206 0.154	0.0123 0.0091 0.00474	97 71 37.1	1 2 3	W310x97 / W12x65 W200x71 / W8x48 W150x37 / W6X25
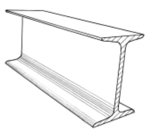 I section rib	0.203 0.152	0.105 0.084	0.00436 0.00236	34 18.6	4 5	S200x 34 / S8x23 S150x18.6 / S6x12.5
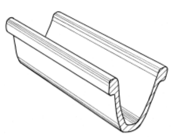 TH section rib	0.148 0.118	0.172 0.135	0.0056 0.0032	44 25	6 7	Toussaint-Heintzmann Profiles
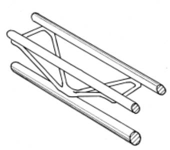 3 bar lattice girder	0.220 0.155	0.191 0.278	0.00197 0.00197	19 18.2	8	Pantex type 130, 26 & 34mm bars Pantex type 95, 26 & 34mm bars
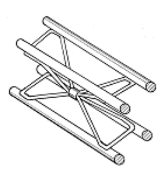 4 bar lattice girder	0.283 0.164	0.220 0.100	0.002828 0.002828	27 25.5	9	Pantex type H1 220, 30 mm bars Pantex type Hi 100, 30 mm bars

Shotcrete or concrete lining	Thickness	Curve number	Rockbolts	Diameter mm	Curve number
	1m 0.3 m 0.15 m 0.1 m 0.05 m	10 11 12 13 14	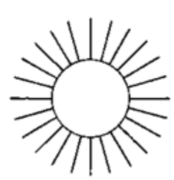	34 25 19 17	15 16 17 18

Figure 12a: Typical examples of support types used in tunnelling.

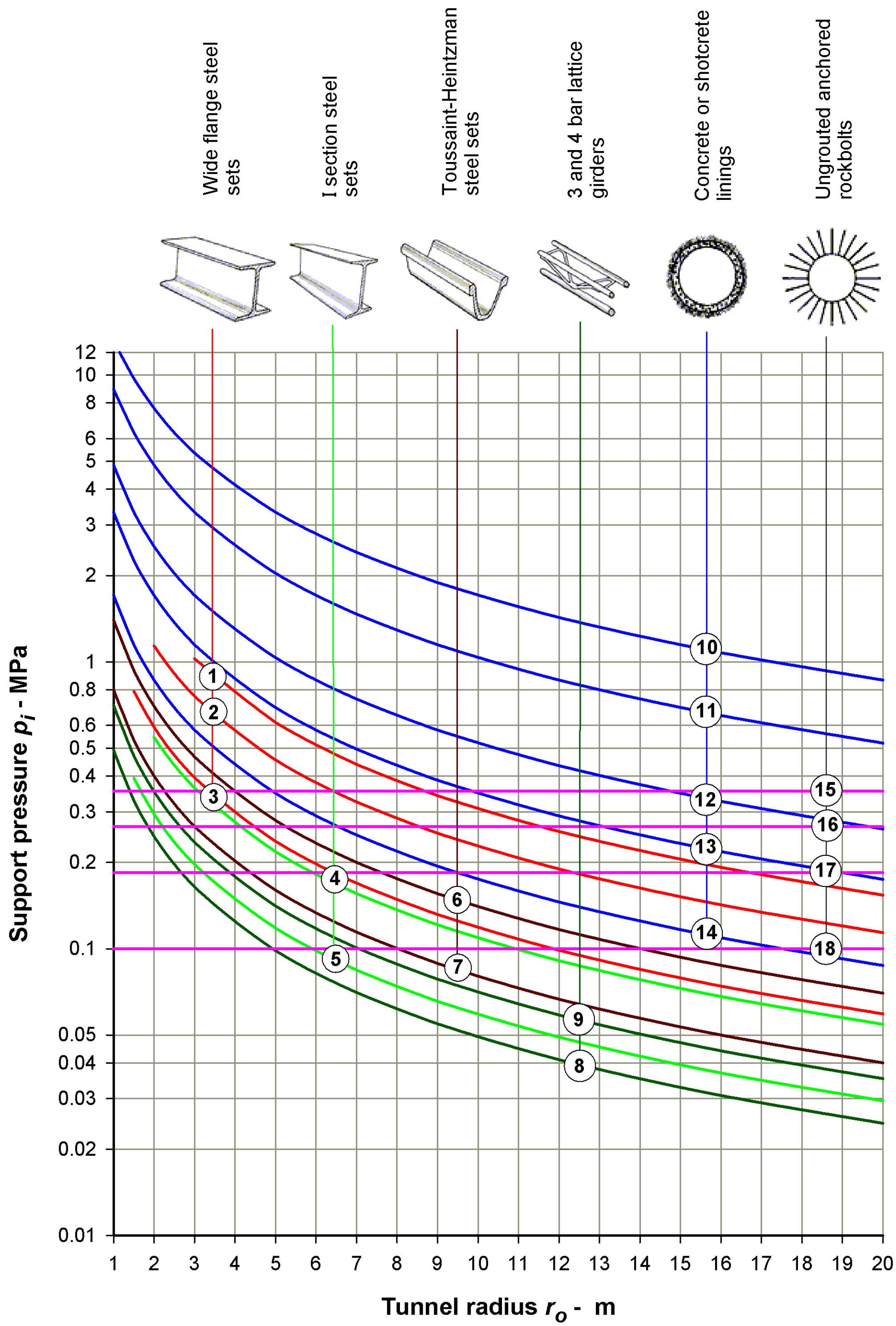

Figure 12b: Maximum support pressure versus tunnel radius for the range of support types defined in Figure 12a.

The following assumptions were made in preparing these plots:

Yield strength of steel components σ_{ys} = 245 MPa
Uniaxial compressive strength of concrete or shotcrete σ_{cc} = 35 MPa
Steel sets are all spaced a 1 m along the tunnel axis
Rockbolts are all placed on a 1 m x 1 m grid pattern.

Note that some of the curves for steel sets are truncated to conform to the normal practice that the bend radius of a steel section should not exceed about 10 times the section depth.

The reader may find it surprising that tunnel radii of up to 20 m are included in Figure 12b. This has been done to show that the support capacity of steel sets and thin shotcrete linings fall to very low levels for large excavation radii. For large underground caverns it is more effective to use rockbolts or cables for support and, even if mesh-reinforced shotcrete is used to hold small rock pieces in place, the support capacity of this shotcrete is ignored in the overall design.

Almost every country involved in tunnelling has its own standards for steel support components and, hence, only a small selection has been included in Figure 12 in order to demonstrate the range of support pressures that can be considered. The reader is advised to consult local structural steel standards and manufacturer specifications for the properties of steel support elements available locally.

Example of rock-support interaction analysis

This example is for the 5 m radius tunnel defined in Figures 4, 6 and 7 with support installed at a distance of 5 m behind the advancing face. As shown in Figure 7, a support pressure of approximately 0.6 MPa is required to stabilize this tunnel and Figure 12b shows that, for a 5 m radius tunnel, this requires W310x97 wide flange steel sets at 1 m spacing or a 0.1m this shotcrete lining. Because of the low stiffness of rockbolt patterns it is difficult to estimate the support performance of rockbolts except by trial and error and a pattern of 34 mm diameter ungrouted end-anchored bolts on a 1 m x 1 m grid spacing will be included in this analysis.

The calculations for the three rock-support interaction curves are given in Figure 13. Note that all three support systems are assumed to act independently and no effort has been made to analyse the support interaction of two or more combined support systems. A plot of the three support curves and their interaction with the characteristic curve for the tunnel is presented in Figure 14.

Both the W310x97 wide flange steel sets, at 1 m spacing, and the 0.3 m thick unreinforced shotcrete lining provide effective support with factors of safety of greater than 2, as shown in Figure 13. The rockbolts do interact with the characteristic curve and give a factor of safety of 2.875. However, their deformation is so large that it is very doubtful that they would be effective in retaining an unravelling rock mass.

Steel sets ***W310x97 (Metric) W12x65 (Imperial) wide flange steel set***

Input:			Output	
Cross sectional area	Ass =	0.0300 m2	Max pss =	1.47 MPa
Steel youngs modulus	Ess =	207000 MPa	uismax =	0.00118 m
Yield strength	Sys =	245 MPa	Stiff. Kss =	1242 MPa/m
tunnel radius	ro =	5 m	strain % =	0.02367
Set spacing along tunnel	Ss =	1 m	Yield uiy =	0.03157 m

Steel set support interaction curve:	x	0.0304	0.0316	0.06
	y	0	1.47	1.47

Approximate Factor of safety for steel set support = 2.1

Shotcrete or concrete ***0.3m thick unreinforced shotcrete***

Input:			Output:	
Young's modulus of concrete	Ecc =	30000 MPa		
Poisson's ration of conctete	gcc =	0.2	Max pscc =	2.037 MPa
Lining thickness	tcc =	0.3 m	uicmax =	0.00526 m
tunnel radius	ro =	5 m	Stiff Kscc	387 MPa/m
UCS of concrete or shotcrete	sconc =	35 MPa	strain % =	0.10528
			Yield uiy =	0.03565 m

Shotcrete lining suport interaction curve:	x	0.0304	0.0357	0.06
	y	0	2.037	2.037

Approximate Factor of safety for shotcrete support = 3.4

Ungrouted rockbolts ***34mm diameter ungrouted end-anchored rockbolts***

Input:			Output	
Free bolt or cable length	Lrb =	3 m		
Diameter of bolt or cable	drb =	0.034 m	Max psr =	0.354 MPa
Young's modulus of bolt or cable	Erb =	207000 MPa	uirmax =	0.00565 m
Ultimate failure load in pull test	Tbfail =	0.354 MN	Stiffness =	63 MPa/m
Tunnel radius	ro =	5 m	strain % =	0.11302
Circumferential bolt spacing	src =	1 m	Yield uiy =	0.03604 m
Longitudinal bolt spacing	srl =	1 m		

Rocbbolt suport interaction curve:	x	0.0304	0.03604	0.06
	y	0	0.354	0.354

Approximate Factor of safety for rockbolt support = 1.0

Figure 13: Rock-support interaction calculations for the example considered.

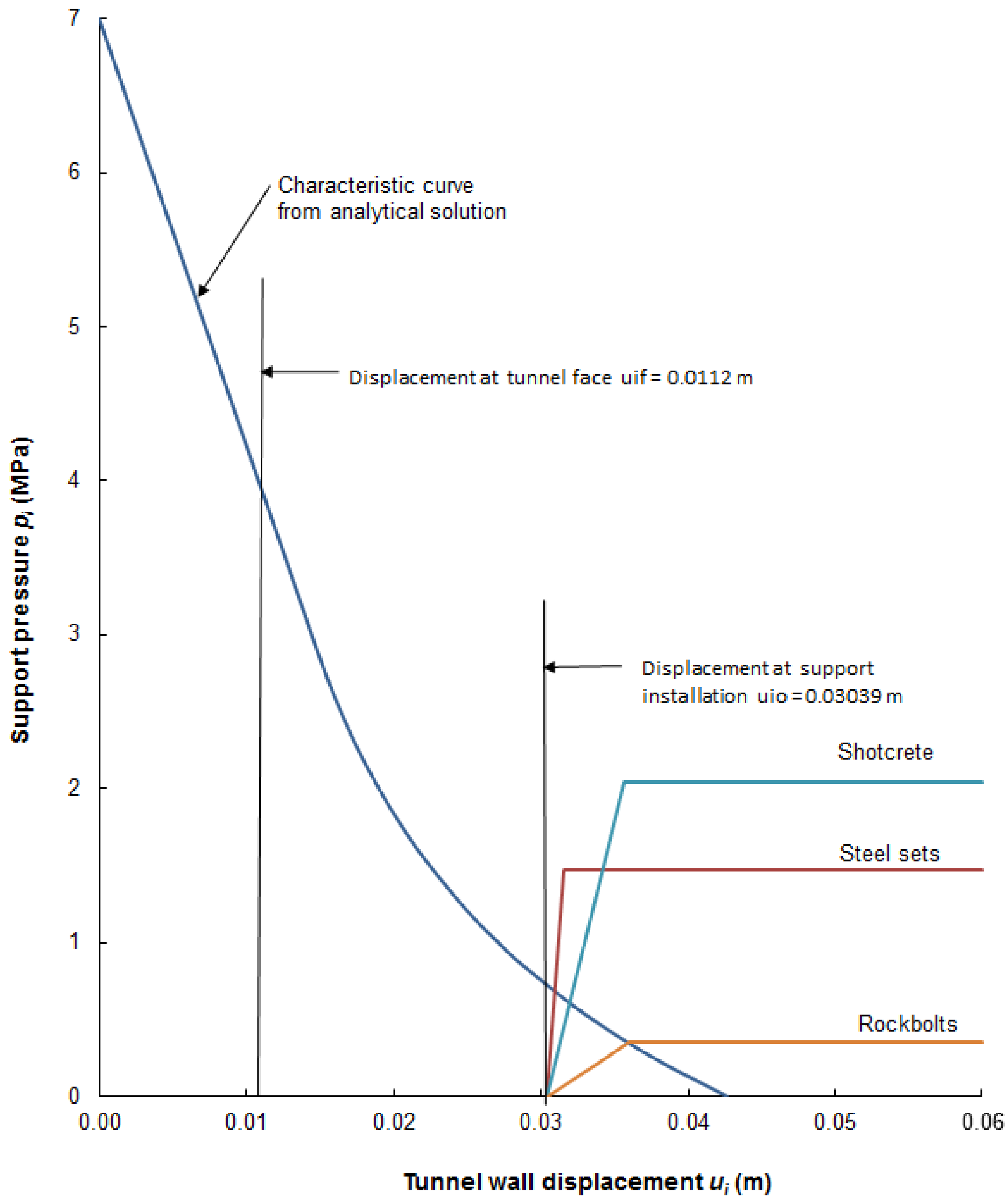

Figure 14: Rock-support interaction plot for the example considered.

Conclusions and recommendations

The rock-support interaction analysis or, as it is sometimes called, the convergence-confinement analyses discussed in these notes is useful for understanding the process of rock mass deformation around an advancing tunnel and the response of support installed inside the tunnel. The analysis demonstrates the importance of tunnel size upon the support capacity of steel sets and shotcrete linings and, in contrast, the lack of sensitivity of rockbolt support to tunnel size. The analysis presented above has been incorporated into the program RocSupport (www.rocscience.com).

The reader should understand that the estimates of the capacity of the support required to stabilize a tunnel are extremely crude as a result of the simplifying assumptions used in the analysis. Remember that the tunnel is assumed to be circular, the in situ stresses are identical in all directions, the rock mass is homogeneous and isotropic and it behaves in elastic-perfectly plastic manner. In an actual tunnel, the profile is very seldom perfectly circular, in in situ stresses are very seldom the same in all directions, the rock mass is generally not homogeneous and isotropic and the failure process is generally far more complex than the elastic-plastic model assumed. In this analysis the calculation of the capacity of the steel sets and the shotcrete lining is based upon the assumption that there are no bending moments or shear forces induced in these support elements and that the loading is characterized by pure axial thrust. The deviations from these simplifying assumptions in an actual tunnel mean that important bending moments and shear forces can be induced in the lining and these may result in premature failure of the support systems.

It is strongly recommended that this analysis should be used as a teaching tool and to give very crude first estimates of possible support requirements. For actual tunnel design use should be made of much more comprehensive analyses such as that published by Hoek et al, 2008, and Carranza-Torres and Diederichs, 2009. These analyses are incorporated into the program Phase2 Version8 (www.rocscience.com).

References

Brady, B.H.G. and Brown, E.T. 1985. *Rock mechanics for underground mining*. London: Allen and Unwin.

Carranza-Torres, C. and Fairhurst, C. 2000. The elasto-plastic response of underground excavations in rock masses that satisfy the Hoek-Brown failure criterion. *International Journal of Rock Mechanics and Mining Sciences 36*(6), 777–809.

Carranza-Torres, C. 2004. Elasto-plastic solution of tunnel problems using the generalized form of the Hoek-Brown failure criterion. Proceedings of the ISRM SINOROCK2004 Symposium China, May 2004. Edited by J.A. Hudson and F. Xia-Ting. *International Journal of Rock Mechanics and Mining Sciences 41*(3), 480–481.

Carranza- Torres, C., and Diederichs, M. 2009. Mechanical analysis of circular liners with particular reference to composite supports. For example, liners consisting of shotcrete and steel sets. *Tunnelling and Underground Space Technology* **24,** 506–532.

Duncan Fama, M.E. 1993. Numerical modelling of yield zones in weak rocks. In *Comprehensive rock engineering*, (ed. J.A. Hudson) **2**, 49-75. Oxford: Pergamon.

Hoek, E., and Brown, E.T. 1980a. *Underground excavations in rock*. London: Instn Min. Metall.

Hoek, E., Carranza-Torres, C., Diederichs, M.S., Corkum, B., 2008. Integration of geotechnical and structural design in tunnelling. In: Proceedings University of Minnesota 56th Annual Geotechnical Engineering Conference, 29 February 2008. Minneapolis, pp. 1–53. Available for downloading at Hoek's Corner at <www.rocscience.com>.

Vlachopoulos**, N**., Diederichs, M.S., 2009. Improved Longitudinal Displacement Profiles for Convergence Confinement Analysis of Deep Tunnels. *Rock Mech.& Rock Eng.*. **42:2,** 131-146.